MULTI-OBJECTIVE OPTIMISATION OF A FREE-FORM BUILDING SHAPE TO IMPROVE THE SOLAR ENERGY UTILISATION POTENTIAL USING ARTIFICIAL NEURAL NETWORKS

XIN ZHAO[1], YUNSONG HAN[2] and LINHAI SHEN[3]
[1,2,3]*School of Architecture, Harbin Institute of Technology; Key Laboratory of Cold Region Urban and Rural Human Settlement Environment Science and Technology, Ministry of Industry and Information Technology, China*
[1]*20S034010@stu.hit.edu.cn* [2]*hanyunsong@hit.edu.cn*
[3]*forestoshen@qq.com*

Abstract. Optimisation of free-form building design is more challenging in terms of building information modelling and performance evaluation compared to conventional buildings. The paper provides a "Photogrammetry-based BIM Modelling - Machine Learning Modelling - Multi-objective Optimisation" framework to improve the solar energy utilisation potential of free-form buildings. Low altitude photogrammetry is used to collect the building and site environmental information. An ANN prediction model is developed using the control point coordinates and simulation data. Through parametric programming, the multi-objective algorithm is coupled with the ANN model to obtain the trade-off optimal building form. The results show that the maximum solar radiation value in winter can increase by 30.60% and the minimum solar radiation in summer can decrease by 13.99%. It is also shown that the integration of ANN modelling and photogrammetry-based BIM modelling into the multi-objective optimisation method can accelerate the optimisation process.

Keywords. Multi-objective optimisation; Artificial neural network; Free-form shape building; Solar energy utilisation.

1. Introduction

Solar radiation is one of the most important factors in building design as it directly affects the heating and cooling energy demand. Solar radiation is even more critical in free-form building design as self-occlusion significantly affects solar energy utilisation. The optimisation of free-form buildings is more time-consuming than that for conventional buildings (Jin and Jeong, 2014) and new optimisation methods are expected to be adopted in the early stages of design.

Multi-objective optimisation models could identify the trade-offs between different and conflicting aspects of potential solutions and provide scientifically sound decision support (Asadi, Silva and Antunes, 2014). There were many studies focused on multi-objective optimisation of buildings. Jin and Jeong

PROJECTIONS, Proceedings of the 26th International Conference of the Association for Computer-Aided Architectural Design Research in Asia (CAADRIA) 2021, Volume 1, 221-230.

(2014) explored the applicability of optimisation methods to minimise the external thermal load of free-form buildings using a genetic algorithm. Zhang, Zhang and Wang. (2016) developed a multi-objective optimisation model to maximise solar radiation and space efficiency and minimise the shape coefficient of a free-form building located in the severe cold region of China. Camporeale and Mercader-Moyano (2019) applied a multi-objective genetic algorithm to modify the high-rise building shape and reduce energy consumption. Ciardiello et al. (2020) proposed a multi-objective approach to optimise the building envelope and reduce energy demand. It is found that building performance can be improved by multi-objective optimisation. However, the process of multi-objective optimisation using simulation data is very time-consuming, particularly when several variables are involved.

Since 2010, many researchers have shown that a machine learning-based model can predict building performance more efficiently than simulation software. In order to reduce the time requirements of the optimisation process, work has been carried out on combining the machine learning model with multi-objective optimisation algorithms. Si et al. (2019) applied different multi-objective optimisation algorithms with ANN models to a newly built tourist centre to improve the indoor thermal comfort and minimise energy demand. Sun, Liu and Han (2020) implemented a multi-objective optimisation design method based on ANN on a public library to improve daylighting, lower energy and operating costs. Seyedzadeh et al. (2020) employed a Random-Forest (RF) model combined with a multi-objective optimisation (MOO) algorithm to predict building heating and cooling loads. Bagheri-Esfeha, Safikhanib and Motahar. (2020) performed multi-objective optimisation using ANN to minimise the heating and cooling loads in a residential building integrated with phase change materials (PCM). These works showed how, with the aid of machine learning models, the process of multi-objective optimisation can be accelerated considerably. However, these examples generally relate to residential buildings which are usually in regular form and there is very limited research focused on the optimisation of free-form buildings. Research that combines multi-objective optimisation and artificial neural networks with solar energy utilisation in severe cold areas is also limited. Moreover, there is still an issue with the heavy time requirements for BIM modelling and the accuracy of this process cannot be guaranteed.

The purpose of the paper is to develop a novel multi-objective optimisation method combining photogrammetry-based BIM modelling, machine learning modelling and multi-objective algorithms to improve the solar radiation utilisation of a free-form building.

2. Methodology

The framework of the proposed method consists of the three steps as shown in Figure 1. The first step is photogrammetry-based BIM modelling. Low altitude photogrammetry is used to collect the building and site environmental information, and a parametric model of the built environment is generated in Grasshopper.

The second step is ANN-based prediction modelling. The structure of the ANN

model is proposed according to the optimisation objective and decision variables. Latin Hypercube Sampling (LHS) is used to generate the input dataset used to train the ANN model. The simulation tools calculate the solar radiation for each group of input datasets, providing the output from the ANN-based prediction model. The ANN is then trained, validated and tested based on the input and output datasets generated in the above steps.

The third step is the performance-driven optimisation process. The multi-objective engine, Wallacei, is launched to conduct the multi-objective optimisation and calculate the optimal solutions coupled with the ANN model.

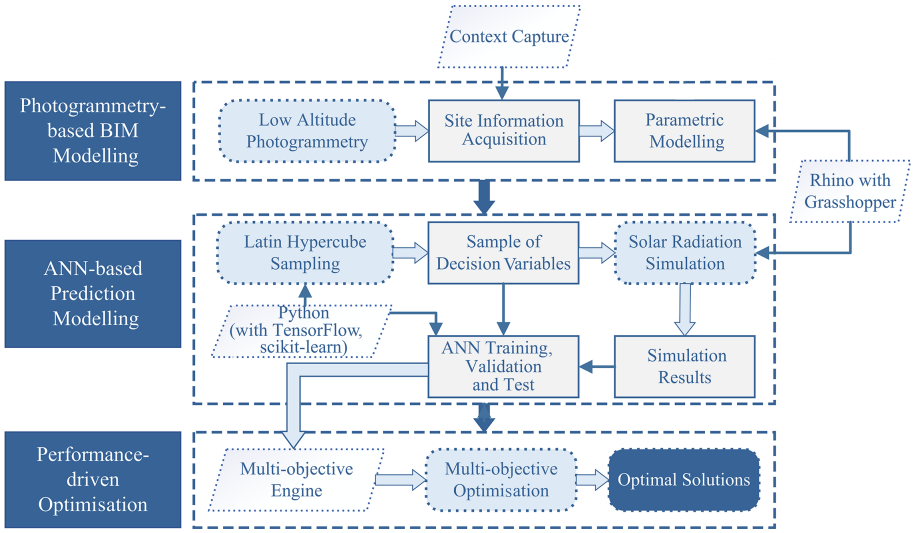

Figure 1. The framework of the proposed method.

2.1. LOW ALTITUDE PHOTOGRAMMETRY AND BIM MODELLING

An Unmanned Aerial Vehicle (UAV) mounted with a camera is used to collect the building and site environmental information. A point cloud can be extracted from the photographs taken by the UAV. A triangular mesh model of the photographed area is then generated, consisting of the surroundings, the target building and the square models. A parametric model of the target building is developed in Rhino and Grasshopper, allowing the coordinates of the main curves (the control points) to be modified to optimise the shape of the building.

2.2. ARTIFICIAL NEURAL NETWORKS

The structure of the ANN used in this work is characterized as a feedforward MLP network. The control-point coordinates are selected as the optimisation variables, and these are also the input variables to the ANN model. A total of 39 input variables are used to represent the variation of the six curves' control points. In order to reduce the size of the training and test dataset while retaining

the characteristics of the data, Latin hypercube sampling (LHS) is used to generate small representative data samples. In this study, 5000 sets of data are generated, each consisting of 39 numbers ranging from 0 to 1.

2.3. MULTI-OBJECTIVE OPTIMISATION

2.3.1. Optimisation objectives

The two optimisation objectives are the maximum solar radiation in winter and the minimum solar radiation in summer, which are contradictory in nature. As the reference building is located in the severe cold zone of China, the maximum solar radiation in winter has a higher weighting.

2.3.2. Decision variables and constraints

The decision variables are the variation of coordinates of the control points which define the main curves and determine the shape of the surfaces.

For a free-form building in the severe cold region, the constraints may arise from the environment which includes the climate and the social conditions including government regulations and standards. The domains and the steps selected for the variation of the variables need to be considered carefully since the appropriate values enable the optimisation process to proceed smoothly and in a reasonable shape.

2.4. PLATFORM

A UAV model is constructed on the Context Capture platform, and the BIM model is built in Rhino and Grasshopper. LHS is implemented using Python. The simulation data used as the output data for the ANN is acquired with the help of Ladybug. The ANN is trained, validated and tested with Python coupled with TensorFlow and the scikit-learn module. The saved ANN model is then loaded into Grasshopper with the help of GH_CPython and the multi-objective optimisation engine, Wallacei is used to calculate the Pareto frontier. The experiments are performed on a computer with a Windows 10 operating system (16 core 3.0GHz processor, 48G RAM).

2.5. REFERENCE BUILDING

The building referenced in this case study is the Harbin Opera House, designed by MAD Architects and located on the Cultural Centre Island of Harbin, China. The building form is composed of free-form surfaces. The distribution of solar radiation on the surface changes with the undulation of the free-form surfaces and is affected by the surrounding environment.

3. Results and discussion

This section illustrates how the proposed method is used to maximise the solar radiation gain in winter and minimise it in summer.

3.1. RESULTS FROM PHOTOGRAMMETRY-BASED BIM MODELLING

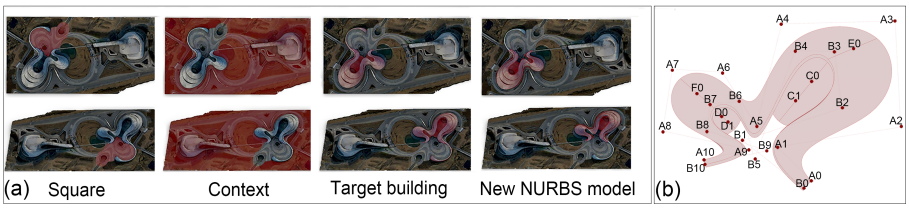

Figure 2. Different parts of photogrammetry-based BIM model and control points of the reference building a) different parts of photogrammetry-based BIM model, b) control points of the reference building.

Table 1. The steps and domains for the movement of the control points.

Curve	Control points	Step			Domain					
		Xstep	Ystep	Zstep	Xmin	Xmax	Ymin	Ymax	Zmin	Zmax
A	A0	1	1	0	20	10	-5	10	——	——
	A1~A8	1	1	0	-25	25	-25	25	——	——
	A9	1	1	0	-25	25	5	10	——	——
	A10	1	1	0	0	20	0	10	——	——
B(points on Curve B move along the vectors between points on Curve A and original points on Curve B)	B0~B4		1			-20			20	
	B5		1			-20			-10	
	B6~B9		1			-25			25	
	B10		1			0			20	
C	C0~C2	——	——	1	——	——	——	——	-30	30
D	D0~D2	——	——	1	——	——	——	——	-10	10
E	E0	——	——	1	——	——	——	——	-30	30
F	F0	——	——	1	——	——	——	——	-10	10

Through low altitude photogrammetry and 3D reconstruction, the UVA model is built. As illustrated in Figure 2, it is divided into three parts on the Rhino and Grasshopper platform, namely the target building, the square and the context, and a new NURBS (non-uniform rational basis spline) surface is modelled. The model is defined by 6 curves with a total of 39 control points. The variation of the points provides the input variables to the ANN and the decision variables for multi-optimisation. The steps and domains for the variation of the control points are shown in Table 1.

3.2. RESULTS OF ARTIFICIAL NEURAL NETWORK MODELLING

3.2.1. Data acquisition and pre-processing

Through LHS and data pre-processing on the Grasshopper platform, random numbers are mapped to the range of each of the optimisation variables and they are used as the input data for the ANN. All of the simulation cases are run in Grasshopper using Ladybug. The simulation of the 5000 cases took around a day. The results of the simulation are written to an Excel file and used as the output data for the ANN training and validation set.

3.2.2. Artificial neural network training, validation and testing

In this study, the ANN is composed of 39 neurons in the input layer, which consists of the variations of the control points, one hidden layer, and one output layer composed of 2 neurons which are the data of the solar radiation.

The input data is scaled to a smaller range using Z-score standardisation defined as follows:

$$Xscale = \frac{x - \mu}{\sigma} \tag{1}$$

where μ and σ represent the average and standard deviation of the input data. The three layers use ReLU as the activation function and the training process uses the Adam optimisation algorithm to update weights.

The dataset is split into 3000 datapoints for training, 1000 for validation and 1000 for testing. The mean squared error (MSE) function is used to evaluate the predictive accuracy of the ANN model defined as follows:

$$MSE = \frac{1}{m}\sum_{i=1}^{m}(y_i - \hat{y}_i)^2 \tag{2}$$

where m = the size of the test set, y_i = the solar radiation simulation value and $\hat{y}_i$ = the predicted value of ANN.

The coefficient of determination(R^2) is used to assess the strength of the correlation of the prediction values and the simulation values, and this usually ranges from 0 to 1. The closer R^2 is to 1, the greater the correlation between the predicted value and the simulated value. R^2 is generally defined as follows:

$$R^2 = 1 - \frac{\sum_{i=1}^{m}(y_i - \hat{y}_i)^2}{\sum_{i=1}^{m}(y_i - \overline{y})^2} \tag{3}$$

where y_i and $\hat{y}_i$ have the same meanings as in (2), and $\overline{y}$= the average value of the set of y_i.

3.2.3. ANN results and discussion

After tuning the parameters on the validation set, the final parameters for training are determined as follows: the number of hidden units is 20, and the dropout rate for both the hidden and the output layer is 0.2, the learning rate is 0.001, epochs are 400, and the batch size is 10. The ANN model reached its goal after approximately 300 epochs, and the final MSE and R^2 values for the training, test and validation sets are shown in Table 2. The final MSE and R^2 for the validation set are 0.299 and 0.992, and the final MSE and R^2 for the training set are 0.303 and 0.992. The MSE and R^2 for the test set are 0.286 and 0.829.

The learning curve demonstrating the MSE and R^2 trends during the training process and the regression between the ANN predictions and the simulation data are illustrated in Figure 3. A good match between the prediction and the simulation data can be seen. To further illustrate the accuracy of the ANN model, Figure 4 compares the 1000 prediction values generated by the ANN model with the winter and summer simulation values. It can be seen that the two data sets are very similar

in both winter and summer.

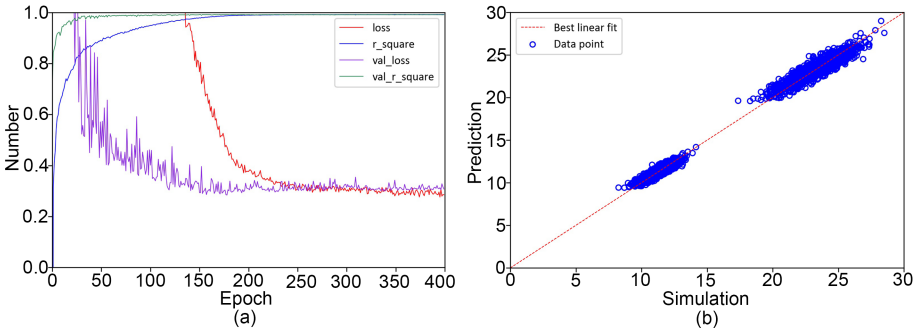

Figure 3. The learning curve and the linear regression between the simulation and prediction values. a) The learning curve, b) Linear regression between the simulation and prediction values.

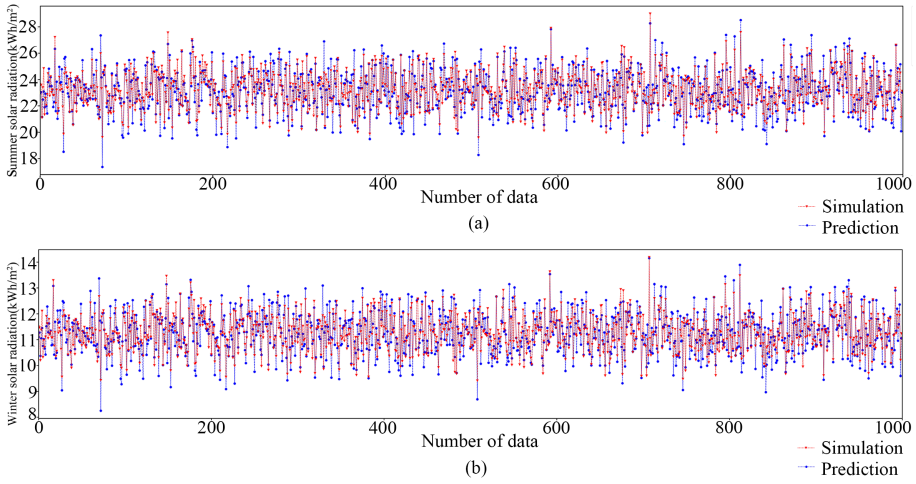

Figure 4. Comparison of ANN prediction and simulation values in summer and winter. a) summer solar radiation, b) winter solar radiation.

Table 2. The final MSE and #R^2# values for the training, test and validation sets.

	MSE	R^2
Training set	0.299	0.992
Validation set	0.303	0.992
Test set	0.286	0.829

3.3. MULTI-OBJECTIVE OPTIMISATION

3.3.1. Multi-objective optimisation settings

After evaluation and testing, the ANN model is used to predict the solar radiation of the reference building for optimisation. For this case, the following GA parameter values are set as shown in Table 3. The generation count is 100, the generation size is 50, crossover probability is 0.9 and mutation probability is 1/r where r represents the number of variables, 39 in this case. The mutation rate is 0.4 and elitism is also 0.4.

Table 3. The GA parameters.

Genetic algorithm parameters	Generation count	Generation size	Crossover probability	Mutation probability	Mutation rates	Elitism	Iteration
Value	100	50	0.9	1/39	0.4	0.4	100

3.3.2. Optimisation results and analysis

With the acceleration of the ANN model, multi-objective optimisation took 6.42 hours. This is considerably less than when just using the simulation data as the optimisation objectives. After 100 iterations, 473 non-dominated solutions are generated. In theory, all of the solutions on the Pareto frontier can be used as final design solutions. To balance the two objectives, 6 non-dominated solutions are chosen for analysis. The results showing the optimised shapes and solutions are shown in Table 4. Solution 5 and Solution 6 have the maximum and minimum solar radiation in summer and winter respectively, and Solutions 1 to 4 are somewhere in between. The solar radiation is 23.59 kWh/m^2 in winter and 11.17 kWh/m^2 in summer for the initial state. The solar radiation in winter is 14.95 kWh/m^2 for Solution 5, which is 30.60% higher than the pre-optimisation state, and value in summer is 30.10 kWh/m^2, 27.60% higher than the initial state. The solar radiation in winter for Solution 6 is 9.69 kWh/m^2, a drop of 12.25%, and the solar radiation in summer is 20.29 kWh/m^2, a reduction of 13.99%. Solutions 1 to 4 are similar. With Solution 1 as an example, solar radiation is 26.07 kWh/m^2 in summer, 10.50% above the initial state while lower than the value for Solution 5, and 12.91 kWh/m^2 in winter, 15.58% higher than the initial state and again lower than Solution 5.

The change in solar radiation varies for the selected solutions, and so does the form of the building. The shape tends to expand both in plan and section to reduce self-occlusion and receive more solar radiation. In the optimisation, the two objectives are contradictory, as lower summer radiation gains results in lower winter solar radiation too. As this reference building is in a severe cold zone in China, the maximisation of winter solar radiation is more important. Hence, a solution with a greater increase in solar radiation in winter and summer, such as Solution 4, is more likely to be selected in a practical application. During the process of optimisation, the variables are modified dynamically to achieve a more reasonable shape. The optimisation process automatically shifts the form in different directions and this can provide support during the early stages of design.

Table 4. Optimisation results and solutions.

solutions		Summer	Winter
	initial state	23.59kWh/m^2	11.17kWh/m^2
1	Area 26726.76m^2	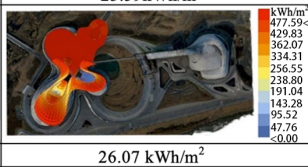	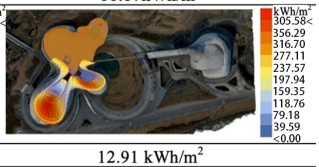
	Radiation value	26.07 kWh/m^2	12.91 kWh/m^2
	Comparison with initial state	10.50%	15.58%
2	Area 32930.87m^2		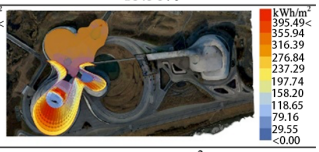
	Radiation value	25.07 kWh/m^2	11.34 kWh/m^2
	Comparison with initial state	6.27%	1.50%
3	Area 27553.18m^2		
	Radiation value	24.79 kWh/m^2	12.38 kWh/m^2
	Comparison with initial state	5.09%	10.83%
4	Area 28368.53m^2		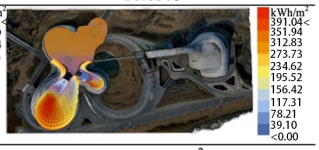
	Radiation value	28.13 kWh/m^2	14.18 kWh/m^2
	Comparison with initial state	19.25%	26.94%
5	Area 29498.04m^2		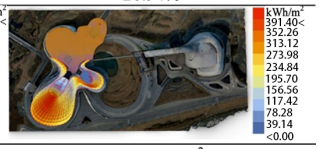
	Radiation value	30.10 kWh/m^2	14.95 kWh/m^2
	Comparison with initial state	27.60%	30.60%
6	Area 27809.81m^2	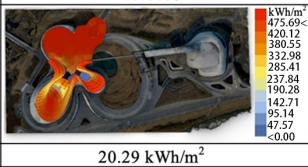	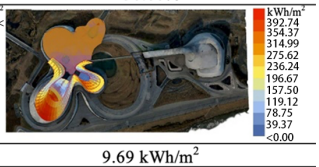
	Radiation value	20.29 kWh/m^2	9.69 kWh/m^2
	Comparison with initial state	-13.99%	-12.25%

4. Conclusion

The research demonstrates an original multi-objective optimisation method for improving the solar energy utilisation potential of a free-form building. The results show that with the aid of ANN and low altitude photogrammetry, the optimisation time can be reduced considerably. In comparison with the initial

state, the maximum solar radiation value in winter increases by 30.60% and the minimum solar radiation in summer is reduced by nearly 13.99%.

The framework applied in this study can accelerate the optimisation process. It offers support to designers and enhances the decision-making process in the design of free-form buildings. The method can be used for future design of free-form buildings and improves the solar energy utilisation potential. It can also be extended to other similar performance-driven design processes.

Acknowledgments

This work was supported by National Natural Science Foundation of China (grant number 52078157); National Natural Science Foundation of China (grant number 51938003); The China Postdoctoral Science Foundation Funded Project (grant number 2017M621276) and the Heilongjiang Postdoctoral Science Foundation (grant number LBH-Z17076). The corresponding author of the article is Yunsong Han (hanyunsong@hit.edu.cn).

References

Asadi, E., Silva, M., Antunes, C., Dias, L. and Glicksman, L.: 2014, Multi-objective optimization for building retrofit: A model using genetic algorithm and artificial neural network and an application., *Energy and Buildings*, **81**, 444-456.

Bagheri-Esfeh, H., Safikhani, H. and Motahar, S.: 2020, Multi-objective optimization of cooling and heating loads in residential buildings integrated with phase change materials using the artificial neural network and genetic algorithm, *Journal of Energy Storage*, **32**, 1-11.

Camporeale, P.E. and Mercader-Moyano, P.: 2019, Towards nearly Zero Energy Buildings: Shape optimization of typical housing typologies in Ibero-American temperate climate cities from a holistic perspective, *Solar Energy*, **193**, 738-765.

Ciardiello, A., Rosso, F., Dell'Olmo, J., Ciancio, V., Ferrero, M. and Salata, F.: 2020, Multi-objective approach to the optimization of shape and envelope in building energy design Adriana, *Applied Energy*, **280**, 115984.

Jin, J. and Jeong, J.: 2014, Optimization of a free-form building shape to minimize external thermal load using genetic algorithm., *Energy and Buildings*, **85**, 473-482.

Seyedzadeh, S., Rahimian, F.P., Oliver, S., Glesk, I. and Kumar, B.: 2020, Data driven model improved by multi-objective optimisation for prediction of building energy loads, *Automation in Construction*, **116**, 103188.

Si, B., Wang, J., Yao, X., Shi, X., Jing, X. and Zhou, X.: 2019, Multi-objective optimization design of a complex building based on an artificial neural network and performance evaluation of algorithms, *Advanced Engineering Informatics*, **40**, 93-109.

Sun, C., Liu, Q. and Han, Y.: 2020, Many-Objective Optimization Design of a Public Building for Energy, Daylighting and Cost Performance Improvement, *Applied Sciences*, **10**, 2435.

Wong, S., Wan, K. and Lam, T.: 2010, Artificial neural networks for energy analysis of office buildings with daylighting., *Applied Energy*, **87(2)**, 551-557.

Zhang, L., Zhang, L. and Wang, Y.: 2016, Shape optimization of free-form buildings based on solar radiation gain and space efficiency using a multi-objective genetic algorithm in the severe cold zones of China, *Solar Energy*, **132**, 38-50.